

The Active-Site Structure of Umecyanin, the Stellacyanin from Horseradish Roots

Christopher Dennison* and Mark D. Harrison

Contribution from the School of Natural Sciences, Bedson Building, University of Newcastle upon Tyne, Newcastle upon Tyne, NE1 7RU, U.K.

Received July 25, 2003; E-mail: christopher.dennison@ncl.ac.uk

Abstract: The type 1 copper sites of cupredoxins typically have a His₂Cys equatorial ligand set with a weakly interacting axial Met, giving a distorted tetrahedral geometry. Natural variations to this coordination environment are known, and we have utilized paramagnetic ¹H NMR spectroscopy to study the active-site structure of umecyanin (UMC), a stellacyanin with an axial Gln ligand. The assigned spectra of the Cu(II) UMC and its Ni(II) derivative [Ni(II) UMC] demonstrate that this protein has the typical His₂Cys equatorial coordination observed in other structurally characterized cupredoxins. The NMR spectrum of the Cu(II) protein does not exhibit any paramagnetically shifted resonances from the axial ligand, showing that this residue does not contribute to the singly occupied molecular orbital (SOMO) in Cu(II) UMC. The assigned paramagnetic ¹H NMR spectrum of Ni(II) UMC demonstrates that the axial Gln ligand coordinates in a monodentate fashion via its side-chain amide oxygen atom. The alkaline transition, a feature common to stellacyanins, influences all of the ligating residues but does not alter the coordination mode of the axial Gln ligand in UMC. The structural features which result in Cu(II) UMC possessing a classic type 1 site as compared to the perturbed type 1 center observed for other stellacyanins do not have a significant influence on the paramagnetic ¹H NMR spectra of the Cu(II) or Ni(II) proteins.

Introduction

Single domain proteins possessing a type 1 copper site (cupredoxins) are an important class of electron-transfer (ET) proteins found in both prokaryotes and eukaryotes.¹ The architecture of the mononuclear metal center of these proteins is key to their biological activity. Crystallographic studies on various cupredoxins have demonstrated that their copper sites usually have a distorted tetrahedral geometry with strong ligands provided by the thiolate sulfur of a Cys and the imidazole nitrogens of two His residues.^{2–12} The active-site structure is typically completed by an unusually long bond to an axial Met ligand [it should be noted that in azurin the backbone carbonyl oxygen of a Gly residue is found 2.6 Å from Cu(II), resulting

in a five-coordinate site with a trigonal bipyramidal geometry¹²]. The residue at the axial position varies, and when cupredoxin domains are found as part of larger protein structures, such as in fungal laccases, the Met can be replaced by a noncoordinating residue such as Phe¹³ or Leu,¹⁴ resulting in a trigonal copper center. The stellacyanins are the only naturally occurring cupredoxins which do not possess an axial Met ligand.^{1,9,15–19} In these proteins, the axial ligand is a Gln residue which coordinates via its side-chain amide oxygen atom (see Figure 1).^{9,19,20} Great interest remains in natural variations to the typical type 1 copper coordination environment as their influence on ET reactivity is not understood.

The stellacyanins form a subclass of a family of cupredoxins called the phytocyanins^{1,17,18} which are probably found in all vascular seed plants^{17,18} and have a number of unusual structural features as compared to other cupredoxins.^{9,10,24} These include

- (1) Nersissian, A. M.; Shipp, E. L. *Adv. Protein Chem.* **2002**, *60*, 271–340.
- (2) Colman, P. M.; Freeman, H. C.; Guss, J. M.; Murata, M.; Norris, V. A.; Ramshaw, J. A. M.; Venkatappa, M. P. *Nature* **1978**, *272*, 319–324.
- (3) Guss, J. M.; Freeman, H. C. *J. Mol. Biol.* **1983**, *169*, 521–563.
- (4) Petratos, K.; Banner, D. W.; Beppu, T.; Wilson, K. S.; Tsernoglou, D. *FEBS Lett.* **1987**, *218*, 209–214.
- (5) Baker, E. N. *J. Mol. Biol.* **1988**, *203*, 1071–1095.
- (6) Nar, H.; Messerschmidt, A.; Huber, R.; van de Kamp, M.; Canters, G. W. *J. Mol. Biol.* **1991**, *221*, 765–772.
- (7) Romero, A.; Nar, H.; Huber, R.; Messerschmidt, A.; Kalverda, A. P.; Canters, G. W.; Durley, R.; Mathews, F. S. *J. Mol. Biol.* **1994**, *236*, 1196–1211.
- (8) Walter, R. L.; Ealick, S. E.; Friedman, A. M.; Blake, R. C.; Proctor, P.; Shoham, M. *J. Mol. Biol.* **1996**, *263*, 730–751.
- (9) Hart, P. J.; Nersissian, A. M.; Herrmann, R. G.; Nalbandyan, R. M.; Valentine, J. S.; Eisenberg, D. *Protein Sci.* **1996**, *5*, 2175–2183.
- (10) Guss, J. M.; Merritt, E. A.; Phizackerley, R. P.; Freeman, H. C. *J. Mol. Biol.* **1996**, *262*, 686–705.
- (11) Bond, C. S.; Blankenship, R. E.; Freeman, H. C.; Guss, J. M.; Maher, M. J.; Selvaraj, F. M.; Wilce, M. C. J.; Willingham, K. M. *J. Mol. Biol.* **2001**, *306*, 47–67.
- (12) Crane, B. R.; Di Bilio, A. J.; Winkler, J. R.; Gray, H. B. *J. Am. Chem. Soc.* **2001**, *123*, 11623–11631.

- (13) Bertrand, T.; Jolival, C.; Briozzo, T.; Caminade, E.; Joly, N.; Madzak, C.; Mougou, C. *Biochemistry* **2002**, *41*, 7325–7333.
- (14) Hakulinen, N.; Kiiskinen, L. L.; Kruus, K.; Saloheimo, M.; Paananen, A.; Koivula, A.; Rouvinen, J. *Nat. Struct. Biol.* **2002**, *9*, 601–605.
- (15) Peisach, J.; Levine, W. G.; Blumberg, W. E. *J. Biol. Chem.* **1967**, *242*, 2847–2858.
- (16) Bergman, C.; Gandvik, E.-A.; Nyman, P. O.; Strid, L. *Biochem. Biophys. Res. Commun.* **1977**, *77*, 1052–1059.
- (17) Nersissian, A. M.; Immoos, C.; Hill, M. G.; Hart, P. J.; Williams, G.; Herrmann, R. G.; Valentine, J. S. *Protein Sci.* **1998**, *7*, 1915–1929.
- (18) Dennison, C.; Harrison, M. D.; Lawler, A. T. *Biochem. J.* **2003**, *371*, 377–383.
- (19) Fields, B. A.; Guss, J. M.; Freeman, H. C. *J. Mol. Biol.* **1991**, *222*, 1053–1065.
- (20) Vila, A. J.; Fernández, C. O. *J. Am. Chem. Soc.* **1996**, *118*, 7291–7298.
- (21) Kraulis, P. J. *J. Appl. Crystallogr.* **1991**, *24*, 946–950.
- (22) Mann, K.; Schäfer, W.; Thoenes, U.; Messerschmidt, A.; Mehrabian, Z.; Nalbandyan, R. *FEBS Lett.* **1992**, *314*, 220–223.

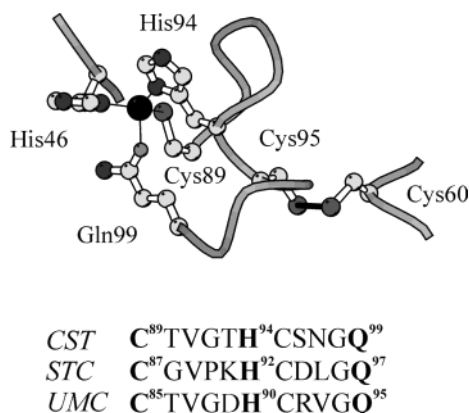


Figure 1. The active-site structure of *C. sativus* stellacyanin (PDB entry 1JER⁹) drawn with MOLSCRIPT.²¹ The C-terminal ligand-containing loop and the disulfide bridge linking Cys60 and Cys95 are included. The alignment of the amino acid sequences of the C-terminal loops of *C. sativus* stellacyanin (CST),²² *R. vernicifera* stellacyanin (STC),¹⁶ and UMC²³ is also shown.

a twist in one of the β -sheets that makes up the β -barrel, a disulfide bridge close to the active site (see Figure 1), and solvent accessibility of the imidazole rings of both histidine ligands. The phytocyanins have been divided into three subgroups (stellacyanins, uclacyanins, and plantacyanins) on the basis of domain organization, glycosylation, and the nature of the axial ligand (the plantacyanins have an axial Met ligand like most other cupredoxins).¹⁷ Stellacyanins are identified by the presence of an axial glutamine ligand, associated carbohydrate, and a cell wall anchoring domain. Umecyanin (UMC) is a stellacyanin isolated from *Armoracia laphatifolia* (horseradish) roots,²⁵ and its axial ligand is the side chain of Gln95 (see Figure 1).²³ UMC is slightly unusual in that it possesses a classic type 1 copper site (low absorbance at ~ 450 nm and an axial EPR spectrum),²⁶ whereas all other stellacyanins, except the *Arabidopsis thaliana* protein (BCB),²⁷ have perturbed type 1 centers (see Figure S1).^{15,18,28–31}

The crystal structure of only one stellacyanin is currently available.⁹ Paramagnetic proton nuclear magnetic resonance (¹H NMR) spectroscopy has been used to study the active-site structures of Cu(II) stellacyanins^{18,26,27,32,33} and also Co(II)^{20,32} and Ni(II)³⁴ derivatives. The NMR investigations have provided detailed information, and the studies on the substituted forms

of *Rhus vernicifera* stellacyanin highlight the axial coordination by a Gln ligand.^{20,34} We have chosen to study the active-site structure of UMC by paramagnetic ¹H NMR spectroscopy utilizing both the Cu(II) and also the Ni(II)-substituted proteins. The aims of this investigation are to confirm that the axial ligand at the type 1 copper site of UMC is a Gln, to assess if there are any significant differences at the active site of UMC as compared to other stellacyanins, and also to determine the influence of the alkaline transition on the active-site structure of UMC.

Materials and Methods

Protein Isolation and Purification. *E. coli* BL21 (DE3) cells were transformed with a pET11a derivative harboring an artificial coding region for the 106 amino acid residue cupredoxin domain of UMC (Glu1 to Gly106),²³ which was synthesized as described elsewhere.²⁷ Overexpression, refolding, and purification of UMC were as described elsewhere.²⁷ Recombinant UMC has spectroscopic properties identical to those of the native protein.²⁷ For the preparation of apo-protein (apo-UMC), the final refolding solution was supplemented with 0.5 mM ethylenediaminetetraacetic acid (EDTA). The apo-UMC was captured by batch binding onto (diethylamino)ethyl (DEAE) Sepharose (Amersham Pharmacia Biotech) and eluted with 25 mM tris-(hydroxymethyl)aminomethane (Tris) pH 7.5 containing 2 M NaCl and 0.5 mM EDTA. Excess salt was removed by dialysis against 25 mM Tris pH 7.5 (containing 0.1 mM EDTA), and the apo-UMC was applied to a DEAE Sepharose column equilibrated in 25 mM Tris pH 7.5 containing 0.1 mM EDTA. The apo-UMC was eluted with a 0–0.4 M NaCl gradient in 25 mM Tris pH 7.5 containing 0.1 mM EDTA and exchanged into 25 mM Tris pH 7.5 by ultrafiltration (Amicon stirred cell, 5 kDa MWCO membrane). To introduce Ni(II) into apo-UMC, a 5-fold molar excess of Ni(NO₃)₂ was added, and the sample was incubated at 4 °C. Nickel uptake was monitored by ultraviolet/visible (UV/vis) spectroscopy and was found to be complete after 48 h. The excess Ni(II) was removed by ultrafiltration, and Ni(II)-substituted UMC [Ni(II) UMC] was further purified by gel filtration chromatography (Superdex 75, Amersham Pharmacia Biotech) in 25 mM Tris pH 7.5 plus 200 mM NaCl. The stellacyanin from *R. vernicifera* was isolated and purified as described previously.¹⁸ The molar extinction coefficients of the proteins were determined as described elsewhere.²⁷

UV/Vis Spectra. UV/vis spectra were acquired on a Perkin-Elmer λ 35 spectrophotometer at 25 °C with the proteins in 10 mM phosphate.

Samples for Paramagnetic ¹H NMR Studies. Paramagnetic ¹H NMR spectra of Cu(II) UMC were obtained with the protein (~ 5 mM) in 37 mM phosphate buffer in both 99.9% D₂O at pH* 7.6 (pH* indicates a pH reading uncorrected for the deuterium isotope effect) and in 90% H₂O/10% D₂O at pH 7.6 and 4.6. To assign the paramagnetic ¹H NMR spectrum of Cu(II) UMC, saturation transfer spectra were obtained on a mixture of Cu(II) and Cu(I) UMC in 37 mM phosphate buffer at pH* 7.6 in 99.9% D₂O. For these experiments, the [Cu(II)] was 1.8 mM and the [Cu(I)] was 3.4 mM. Paramagnetic NMR spectra of Ni(II) UMC were obtained with the protein (~ 5 mM) in 10 mM phosphate in 99.9% D₂O at pH* 8.0 and in 90% H₂O/10% D₂O in the pH range 5.6–10.8. It should be noted that at high protein concentrations Ni(II) UMC was not stable at pH values below 6.5 and above 10.5.

NMR Spectroscopy. All proton NMR spectra were acquired either at 500.16 MHz on a JEOL Lambda 500 spectrometer or at 300.13 MHz on a Bruker Avance 300 spectrometer as described previously.^{35,36} The

- (23) Van Driessche, G.; Dennison, C.; Sykes, A. G.; Van Beeumen, J. *Protein Sci.* **1995**, *4*, 209–227.
 (24) Einsle, O.; Mehrabian, Z.; Nalbandyan, R.; Messerschmidt, A. *J. Biol. Inorg. Chem.* **2000**, *5*, 666–672.
 (25) Paul, K. G.; Stigbrand, T. *Biochim. Biophys. Acta* **1970**, *221*, 255–263.
 (26) Dennison, C.; Lawler, A. T. *Biochemistry* **2001**, *40*, 3158–3166.
 (27) Harrison, M. D.; Dennison, C. *Proteins: Struct. Funct. Genet.*, in press.
 (28) Nersissian, A. M.; Mehrabian, Z. B.; Nalbandyan, R. M.; Hart, P. J.; Fraczkiewicz, G.; Czernuszewicz, R. S.; Bender, C. J.; Peisach, J.; Herrmann, R. G.; Valentine, J. S. *Protein Sci.* **1996**, *5*, 2184–2192.
 (29) Andrew, C. R.; Yeom, H.; Valentine, J. S.; Karlsson, B. G.; Bonander, N.; van Pouderooyen, G.; Canters, G. W.; Loehr, T. M.; Sanders-Loehr, J. *J. Am. Chem. Soc.* **1994**, *116*, 11489–11498.
 (30) LaCroix, L. B.; Randall, D. W.; Nersissian, A. M.; Hoitink, C. W. G.; Canters, G. W.; Valentine, J. S.; Solomon, E. I. *J. Am. Chem. Soc.* **1998**, *120*, 9621–9631.
 (31) DeBeer, G. S.; Basumallick, L.; Szilagyi, R. K.; Randall, D. W.; Hill, M. G.; Nersissian, A. M.; Valentine, J. S.; Hedman, B.; Hodgson, K. O.; Solomon, E. I. *J. Am. Chem. Soc.* **2003**, *125*, 11314–11328.
 (32) Fernández, C. O.; Sannazzaro, A. I.; Vila, A. J. *Biochemistry* **1997**, *36*, 10566–10570.
 (33) Bertini, I.; Fernández, C. O.; Karlsson, B. G.; Leckner, J.; Luchinat, C.; Malmström, B. G.; Nersissian, A. M.; Pierattelli, R.; Shipp, E.; Valentine, J. S.; Vila, A. J. *J. Am. Chem. Soc.* **2000**, *122*, 3701–3707.
 (34) Fernández, C. O.; Sannazzaro, A. I.; Diaz, L. E.; Vila, A. J. *Inorg. Chim. Acta* **1998**, *273*, 367–371.

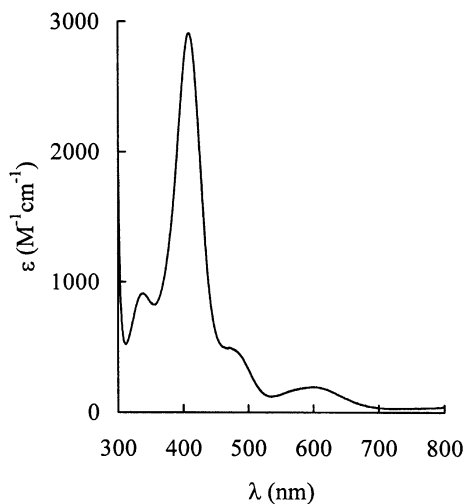
(35) Dennison, C.; Sato, K. *Inorg. Chem.* **2002**, *41*, 6662–6672.

(36) Sato, K.; Kohzuma, T.; Dennison, C. *J. Am. Chem. Soc.* **2003**, *125*, 2101–2112.

Table 1. Wavelengths (nm) and Intensities (ϵ , $M^{-1} \text{ cm}^{-1}$) in Parentheses of the LMCT and LF Transitions in the UV/Vis Spectra of Ni(II)-Substituted Cupredoxins

UMC ^a	STC ^b	M121Q azurin ^c	pseudoazurin ^d	amicyanin ^e	azurin ^f	assignment ^g
338 (930)	335 (1600)	320 (~600)	346 (2180)	342 (1690)	354 (1350)	LMCT
408 (2930)	410 (3500)	416 (~2400)	420 (2850)	428 (2860)	440 (2900)	LMCT
480 (sh) ^h	470 (sh)	480 (sh)	480 (sh)	495 (sh)	490 (sh)	i
560 (100)	550 (400)	550 (<200)	550 (sh)		560 (150)	LF
610 (110)	590 (400)	620 (<200)	680 (150)	690 (140)		LF

^a This study at pH 7.6 and 25 °C. ^b *R. vermifera* stellacyanin at 25 °C, ref 38. ^c The Met121Gln variant of *Alcaligenes denitrificans* azurin at pH 7.0 and 25 °C, ref 40. ^d *Achromobacter cycloclastes* pseudoazurin at pH 8.0 and 25 °C, ref 35. ^e *Paracoccus versutus* amicyanin at pH 8.2 and 25 °C, ref 41. ^f *A. denitrificans* azurin at pH 7.0 and 25 °C, ref 40. ^g As in ref 39. ^h Shoulder. ⁱ Not assigned in ref 39 but previously identified as an LMCT band.^{37,38}

**Figure 2.** UV/vis spectrum (25 °C) of Ni(II) UMC in 10 mM phosphate at pH 7.6.

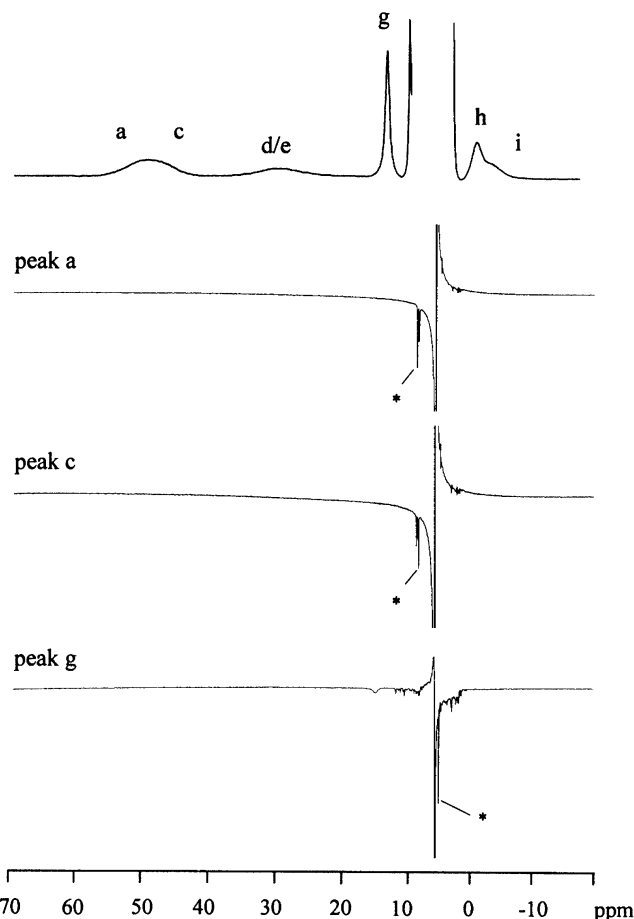
NOE data were analyzed using eq 1 which is valid in the slow-motion limit:

$$\eta_{ij} = -\left(\frac{\mu_0}{4\pi}\right)^2 \left(\frac{\hbar^2 \gamma_H^4 \tau_r}{10r_{ij}^6 \rho_i}\right) \quad (1)$$

where η_{ij} is the NOE observed for signal i upon irradiation of signal j, μ_0 is the magnetic permeability of a vacuum, \hbar is Planck's constant (h) divided by 2π , γ_H is the magnetogyric ratio of the proton, τ_r is the rotational correlation time of the protein (a value of 1×10^{-8} s was used for UMC), r_{ij} is the distance between the protons i and j, and ρ_i is the longitudinal relaxation rate (T_1^{-1}) of proton i.

Results

The UV/Vis Spectrum of Ni(II) UMC. The UV/vis spectrum of Ni(II) UMC at pH 7.6 is shown in Figure 2, and the positions of the absorption bands are listed in Table 1. The positions of peaks in the UV/vis spectra of other Ni(II) cupredoxins^{35,37–41} are also included in Table 1. The UV/vis spectrum of Ni(II) UMC is influenced by the alkaline transition, and the ligand to metal charge-transfer (LMCT) bands are found at 329 and 398 nm at pH 10.6. The broad features at ~560 and 610 nm

**Figure 3.** ¹H NMR saturation transfer difference spectra (500 MHz) of a mixture of Cu(I) (3.4 mM) and Cu(II) (1.8 mM) UMC in 37 mM phosphate (99.9% D₂O) at pH* 7.6 (40 °C). The top spectrum is that of Cu(II) UMC, and those below are the saturation transfer difference spectra in which the peaks indicated were irradiated. The observed saturation transfer peaks in the Cu(I) protein are shown by an asterisk.

are affected by increasing pH, and only a single band centered at around 615 nm is observed at pH 10.6 (data not shown).

The Assignment of the ¹H NMR Spectrum of Cu(II) UMC. The paramagnetic ¹H NMR spectrum of Cu(II) UMC in 99.9% deuterated buffer is shown in Figure 3. The spectrum exhibits two additional exchangeable resonances in 90% H₂O/10% D₂O at acidic pH.²⁶ Therefore, Cu(II) UMC has seven directly observed downfield shifted resonances and two upfield shifted signals. The temperature dependence of the positions of the hyperfine-shifted signals (data not shown) indicates that all of these resonances exhibit Curie-type behavior (increasing shift with decreasing temperature). We have assigned the signals in the spectrum of UMC using saturation transfer experiments on

(37) Tennent, D. L.; McMillin, D. R. *J. Am. Chem. Soc.* **1979**, *101*, 2307–2311.

(38) Lum, V.; Gray, H. B. *Isr. J. Chem.* **1981**, *21*, 23–25.

(39) Di Bilio, A.; Chang, T. K.; Malmström, B. G.; Gray, H. B.; Karlsson, B. G.; Nordling, M.; Pascher, T.; Lundberg, L. G. *Inorg. Chim. Acta* **1992**, *198–200*, 145–148.

(40) Salgado, J.; Jiménez, H. R.; Moratal, J. M.; Kroes, S.; Warmerdam, G. C. M.; Canters, G. W. *Biochemistry* **1996**, *35*, 1810–1819.

(41) Salgado, J.; Kalverda, A. P.; Diederix, R. E. M.; Canters, G. W.; Moratal, J. M.; Lawler, A. T.; Dennison, C. *J. Biol. Inorg. Chem.* **1999**, *4*, 457–467.

Table 2. Hyperfine-Shifted Resonances in the ^1H NMR Spectrum of Cu(II) UMC and Their Diamagnetic Counterparts in the Cu(I) Protein^a

resonance	δ_{obs} (ppm) ^b in Cu(II) UMC	δ_{dia} (ppm) in Cu(I) UMC	assignment	δ_{obs} (ppm) ^b in CST ^c	δ_{obs} (ppm) ^b in STC ^d
a	51	7.49 ^e	His44/90 C ^{δ} 2H	55.0	57
b	~47 ^f	nd ^g	His44/90 N ^e 2H		
c	48	7.20 ^e	His44/90 C ^{δ} 2H	48.0	49
d/e	~30	7.58/7.25 ^e	His44/90 C ^e 1H	41.2/29.8	~30
f	28.5 ^f	nd	His44/90 N ^e 2H	26 ^h	23.7 ⁱ
g	13.7	4.01 ^j	Asp45 C ^{α} H	16.9	14.8
h	-4.2 ^k	nd	His44/90 C ^{β} H		-2
i	~ -6	5.33 ^j	Cys85 C ^{α} H	-7.5	-7.6

^a Data recorded at 40 °C in 37 mM phosphate buffer in 99.9% D₂O at pH* 7.6. Also included are the assignments that have been made and the data for two other stellacyanins. ^b The observed shifts (δ_{obs}) arise from the three contributing factors δ_{dia} , δ_{pc} , and δ_{Fc} [δ_{dia} is the shift in an analogous diamagnetic system, δ_{pc} is the pseudocontact (through-space) contribution, and δ_{Fc} is the Fermi-contact (through-bond) contribution]. The δ_{pc} values are small, due to the small anisotropy of the g tensor, and range from ~3 to -5 ppm.³³ Therefore, δ_{obs} minus δ_{dia} for a particular proton provides a good estimate of δ_{Fc} , which is a measure of the spin density. ^c *C. sativus* stellacyanin at 28 °C and pH 6.0.³³ The residues corresponding to those of UMC which are included in the assignment column are His46, Asn47, Cys89, and His94. ^d *R. vernicifera* stellacyanin recorded at 30 °C and pH 7.0.¹⁸ The residues corresponding to those of UMC which are included in the assignment column are His46, Asn47, Cys87, and His92. ^e The signals at 7.49 and 7.58 ppm can be assigned to the imidazole ring protons of one of the His ligands, and those at 7.20 and 7.25 ppm can be assigned to the other His ligand on the basis of cross-peaks observed in a TOCSY spectrum of Cu(I) UMC. In a NOESY spectrum of Cu(I) UMC, a strong NOE is observed between the signals at 7.58 and 7.25 ppm which can only arise between the C^e1H protons of the two His ligands (assuming coordination via their N^o1 atoms). ^f Resonances from exchangeable protons observed in 90% H₂O/10% D₂O at pH < 6.0. The δ_{obs} values quoted here were measured in 10 mM phosphate 90% H₂O/10% D₂O at pH 4.6 and 25 °C. These signals can arise from either the N^e2H protons of the two His ligands (His44 and His90) or the N^e2H protons of the axial Gln95 ligand. Given that no other shifted resonances are observed from the axial ligand and that these resonances are still present in the spectrum of the Gln95Met UMC variant (data not shown), we can assign these to the His ligands. ^g Not determined. ^h Assigned to His46.³³ ⁱ Measured in 10 mM phosphate 90% H₂O/10% D₂O at pH 4.6 and 25 °C. ^j The δ_{dia} values of signals g and i indicate that they arise from C ^{α} H protons. Previous studies have demonstrated^{33,36,42-44} that the relatively sharp peak at around 15 ppm in the paramagnetic NMR spectra of Cu(II) cupredoxins arises from the C ^{α} H of the Asn residue adjacent to the N-terminal His ligand. The corresponding residue in UMC is Asp45. The C ^{α} H of the Cys ligand is always quite broad and upfield shifted in the spectra of Cu(II) cupredoxins.^{33,36,42-44} ^k Tentatively assigned on the basis of previous investigations.^{33,36,42-44}

Table 3. Hyperfine-Shifted Resonances in the ^1H NMR Spectrum of Ni(II) UMC at 30 °C and pH 8.0^a

resonance	δ_{obs} (ppm)	T_1 (ms)	$\Delta\nu_{1/2}$ (Hz)	assignment
a	224	1.1	900	Cys85 C ^{β} H
b	167	1.0	830	Cys85 C ^{β} H
c	69.5	6.5	170	His44/90 C ^{δ} 2H
d	52.5	8.2	200	His44/90 C ^{δ} 2H
e	57.4 ^b	nd ^c	nd ^c	His44/90 N ^e 2H
f	42.2	8.6	200	Gln95 C ^{γ} H
g	39.5	nd	~600	His44/90 C ^e 1H
h	39.5 ^b	5.1	140	His44/90 N ^e 2H
i	~34	nd	~800	His44/90 C ^e 1H
j	18.3	nd	~1300	
k	-3.1	12	100	Cys85 C ^{α} H
l	-5.4	3	200	His C ^{β} H
m	-17.8	4.0	200	Gln95 N ^e 21H
n	-25.1	10.9	220	Gln95 C ^{γ} H

^a Data recorded at 300 MHz. Also included are the observed chemical shifts (δ_{obs}), the spin lattice (T_1) relaxation times, the peak widths ($\Delta\nu_{1/2}$), and the assignments that have been made. ^b Measured at pH 5.6 and 2 °C. ^c Not determined.

a mixture of the Cu(II) and Cu(I) protein.^{33,36,42-44} The data obtained when irradiating peaks a, c, and g are shown in Figure 3. Listed in Table 2 are the results of all of the saturation transfer experiments and the assignments that have been made for UMC.

The Assignment of the ^1H NMR Spectrum of Ni(II) UMC. The paramagnetic ^1H NMR spectrum of Ni(II) UMC is shown in Figure 4A and B. The observed resonances in the spectrum are listed in Table 3, along with their spin-lattice (T_1) relaxation times and peak widths ($\Delta\nu_{1/2}$). The peaks labeled a-n have properties (hyperfine shifts, line widths, and T_1 values) which identify them as arising from protons associated with the coordinating amino acid residues. The temperature dependence

of the chemical shifts of these resonances was studied in the range 2-45 °C (data not shown), and all signals exhibit Curie-type behavior (increasing shift with decreasing temperature). Furthermore, all of the signals, except peak b, have chemical shifts at infinite temperature which are all close to the diamagnetic region, and thus the δ_{pc} contributions to the observed shifts of most of the shifted resonances are not so significant.

Peaks e, h, and m are exchangeable resonances and therefore can arise from either the N^e2H protons of the two His ligands or the N^e2H protons of the axial Gln95 ligand. Peak m is still observed at pH 10.7, peak e, which overlaps with peak d, is not observed above pH 7.0 but is apparent at pH 6.5 and 10 °C, while peak h is hardly observed under these conditions (see Figure 4B). At low temperature (2 °C) and pH 5.6 (see Figure 5A), the intensity of peak h is equivalent to ~0.5 of a proton, while that of the combined peak d and e is equivalent to two protons (integration was performed on WEFT spectra obtained with long delay times, thus avoiding any problems caused by differences in T_1 values). The behavior of the exchangeable resonances indicates that peaks e and h belong to protons which undergo fast exchange with the bulk solvent (are solvent exposed) whereas peak m arises from a more buried proton. This is consistent with peaks e and h belonging to the N^e2H protons of the His ligands (both His ligands are solvent exposed in the available phytoeyanin crystal structures^{9,10,24}) and with peak m arising from one of the N^e2H protons of the axial Gln95 ligand.

Irradiation of peak c gives rise to an NOE to peak h (see Figure 5C), and the reverse NOE is seen when the latter signal is irradiated (see Figure 5D). The relaxation properties of peak c identify it as arising from the C ^{δ} 2H proton of a His ligand (coordination via the N^o1 atom of a His residue results in the C^e1H proton being very close to the paramagnetic metal and thus its resonance will be broad and have a short T_1 value, whereas the C ^{δ} 2H proton will be much further from the metal

- (42) Kalverda, A. P.; Salgado, J.; Dennison, C.; Canters, G. W. *Biochemistry* **1996**, *35*, 3085-3092.
 (43) Bertini, I.; Ciurli, S.; Dikiy, A.; Gasanov, R.; Luchinat, C.; Martini, G.; Safarov, N. *J. Am. Chem. Soc.* **1999**, *121*, 2037-2046.
 (44) Donaire, A.; Jiménez, B.; Fernández, C. O.; Pierattelli, R.; Niizeki, T.; Moratal, J. M.; Hall, J. F.; Kohzuma, T.; Hasnain, S. S.; Vila, A. J. *J. Am. Chem. Soc.* **2002**, *124*, 13698-13708.

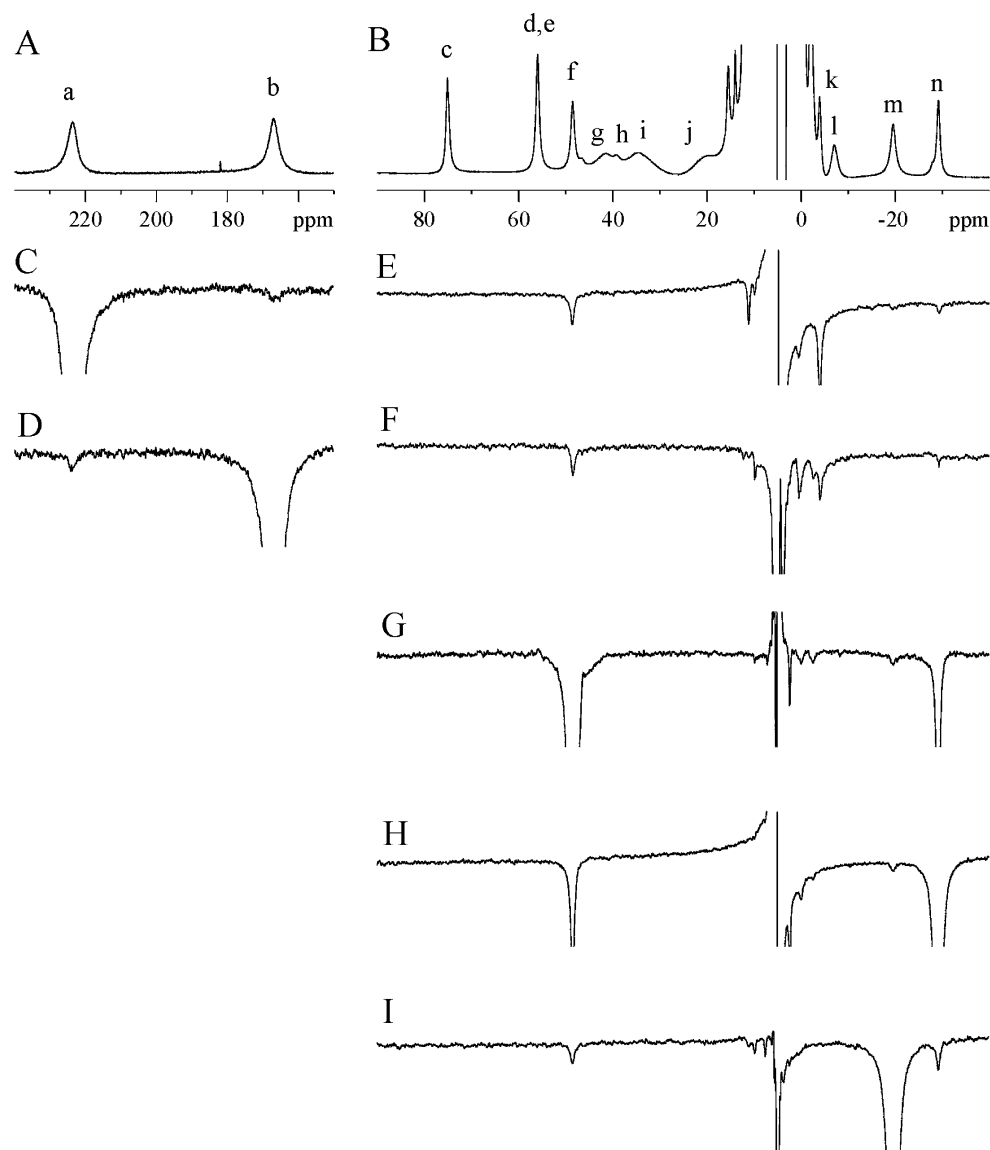


Figure 4. Reference (A and B) and difference (C–I) ^1H NMR spectra (300 MHz) of Ni(II) UMC corresponding to 1D NOE experiments performed in 10 mM phosphate buffer. Spectra A, C, and D were acquired at 30 °C with the sample in 99.9% deuterated buffer at pH* 8.0. Spectra B and E–I were measured at 10 °C with the protein in 90% $\text{H}_2\text{O}/10\%$ D_2O at pH 6.5. In spectra C and E, peak a was irradiated, while in spectra D and F, peak b was irradiated. In spectra G, H, and I, peaks f, n, and m, respectively, were irradiated.

and its signal will be sharper and have a longer T_1). Irradiation of the broad signal i gives rise to an NOE to peak e (see Figure 5E; note: irradiation of peak i in 99.9% D_2O did not give rise to an NOE to peak d), whereas irradiation of the composite signal d/e did not give rise to any NOEs to other isotropically shifted resonances. The properties of peak i indicate that it arises from a $\text{C}^\epsilon\text{H}$ proton of one of the His ligands and peak e and peak d must both belong to this His residue (with peak d arising from the $\text{C}^{\delta 2}\text{H}$ proton). The broad signal g is tentatively assigned to the $\text{C}^\epsilon\text{H}$ proton of the other His ligand (whose $\text{C}^{\delta 2}\text{H}$ and $\text{N}^{\epsilon 2}\text{H}$ resonances are signals c and h, respectively). The NOE between peak g and signal h could not be observed due to the overlap of these two signals in the spectrum of Ni(II) UMC (peak j could be discounted as the other His $\text{C}^\epsilon\text{H}$ proton resonance as irradiation of this signal did not give rise to an NOE to signal h). We have not observed NOEs to or from signal l, but on the basis of the relaxation properties of this resonance, we tentatively assign it as the C^βH proton of one of the His ligands.

The large isotropic shifts and line widths, and the short T_1 values of peaks a and b (see Figure 4A and Table 3), identify them as the C^βH protons of the Cys85 ligand.^{20,34,35,40,41} This is confirmed by the intensity of the observed NOEs between these two peaks (see Figure 4C and D), which are consistent with the T_1 values of these signals and the expected proton–proton distance for geminal protons [expected NOE intensities were calculated using eq 1 and a τ_r value of 1×10^{-8} s]. Irradiation of both peaks a and b results in NOEs to the relatively sharp peak k, which we assign as belonging to the Cys85 C^αH proton, and also to peaks f and n (see Figure 4E and F).

The strong NOEs observed between peaks f and n (see Figure 4G and H) indicate that these signals arise from a geminal pair of protons (this is consistent with the distance between such protons, the T_1 values listed in Table 3, and the NOE intensities observed – see eq 1). NOEs are also observed to the exchangeable signal m (which is one of the $\text{N}^{\epsilon 2}\text{H}$ protons of the axial Gln95 ligand, *vide supra*) upon irradiation of peak f (see Figure 4G) and resonance n (see Figure 4H), and the reverse NOEs to

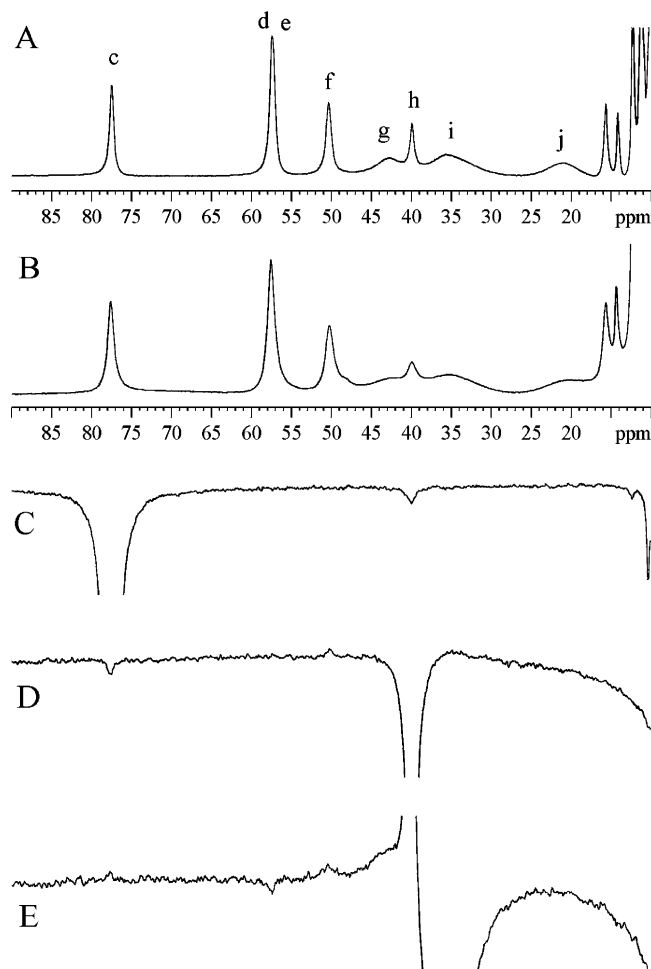


Figure 5. ^1H NMR spectra (300 MHz) of Ni(II) UMC in 10 mM phosphate buffer in 90% $\text{H}_2\text{O}/10\%$ D_2O at 2 $^\circ\text{C}$. In spectrum A, the sample was at pH 5.6, while in (B), the pH is 6.5. (B) is the reference spectrum for the difference spectra also shown (C–E) corresponding to 1D NOE experiments. In spectra C, D, and E, peaks c, h, and i, respectively, were irradiated.

signals f and n are seen upon irradiation of peak m (see Figure 4I). Both peaks f and n give rise to an NOE to the relatively sharp peak at 2.4 ppm. Thus, we confirm that resonance m is one of the $\text{N}^{\epsilon 2}\text{H}$ protons of Gln95 and assign peaks f and n to the $\text{C}^{\gamma}\text{H}$ protons of this residue, and the sharper peak at 2.4 ppm as one of its C^{β}H protons. These assignments are consistent with the NOEs between peaks a and b and resonances f and n (see Figure 4E and F) as the Cys89 C^{β}H protons point toward the Gln99 $\text{C}^{\gamma}\text{H}$ protons in the structure of *Cucumis sativus* (cucumber) stellacyanin⁹ (see Figure 1).

The positions of most signals in the paramagnetic ^1H NMR spectrum of Ni(II) UMC are influenced by pH in the range 8.0–10.7, indicating a pH-dependent equilibrium in which exchange between the two forms is fast on the NMR time scale (see Table 4). The Cys85 C^{β}H protons are most affected, and their average shift ($\delta_{\beta,\text{av}}$) decreases from 196 ppm at pH 8.0 to 170 ppm at pH 10.7. Furthermore, the separation between the δ_{obs} values for the two Cys85 C^{β}H protons decreases from 57 ppm at pH 8.0 to 37 ppm at pH 10.7. The δ_{obs} values of the $\text{C}^{\gamma}\text{H}$ protons of Gln95 decrease at alkaline pH, with a greater effect observed for peak f. The $\text{N}^{\epsilon 2}\text{H}$ signal of the axial Gln ligand (peak m) is still observed at pH 10.7, but its δ_{obs} is not significantly influenced by the alkaline transition. The resonances from the

Table 4. The Observed Hyperfine Shifts (δ_{obs}) in the ^1H NMR Spectrum of Ni(II) UMC As Compared to the δ_{obs} Values for the Corresponding Resonances in Ni(II) *R. vernicifera* Stellacyanin (STC) and Ni(II) M121Q Azurin^a

ligand ^b	proton	δ_{obs} (ppm)	δ_{obs} (ppm)	δ_{obs} (ppm)	δ_{obs} (ppm)
		Ni(II) UMC at pH 8.0 ^c	Ni(II) UMC at pH 10.7 ^c	Ni(II) STC ^d	Ni(II) M121Q azurin ^e
His	$\text{H}^{\delta 2}$	52.5 (50.8) ^f	54.9	52.1	65.1
	$\text{H}^{\epsilon 1}$	~34 (~33)	~33	28.0/39.8	43.5
	$\text{H}^{\epsilon 2}$	57.4 ^g		50.8	33.5
Cys ^h	$\text{H}^{\beta 1}$	167 (163)	151	177	178
	$\text{H}^{\beta 2}$	224 (216)	188	197	237
His	H^{α}	-3.1 (-2.7)			-2.1
	$\text{H}^{\delta 2}$	69.5 (67.1)	70.0	67.1	55.7
	$\text{H}^{\epsilon 1}$	39.5 (38.2)	35.3	28.0/39.8	49.0
Gln ^h	$\text{H}^{\epsilon 2}$	39.5 ^g		33.9	54.1
	$\text{H}^{\epsilon 21}$	-17.8 (-16.9)	-16.9	-18.0 ⁱ	-8.9
	$\text{H}^{\gamma 1}$	42.2 (40.5)	30.9	33.2	37.7
Gly	$\text{H}^{\gamma 2}$	-25.1 (-23.9)	-21.0	-21.0	-8.6
	$\text{H}^{\beta 1}$	2.4		0.5	2.4
	$\text{H}^{\beta 2}$				5.2
Gly	$\text{H}^{\alpha 1}$				28.9
	$\text{H}^{\alpha 2}$				-2.3

^a Also included are the δ_{obs} values for Ni(II) UMC at pH 10.7. ^b From top to bottom; His44, Cys85, His90, and Gln95 for UMC [here, we have assumed that His44 is more buried than His90 in line with the assumption made for Ni(II) STC]; His46, Cys87, His92, and Gln97 for *R. vernicifera* stellacyanin; and His46, Cys112, His117, Gln121, and Gly45 for M121Q azurin. ^c Measured at 30 $^\circ\text{C}$. ^d Measured at pH 4.0 and 40 $^\circ\text{C}$.³⁴ ^e The Met121Gln variant of *A. denitrificans* azurin at pH 5.5 and 30 $^\circ\text{C}$.⁴⁰ ^f The values in parentheses are those measured at 40 $^\circ\text{C}$ (pH 8.0). ^g Measured at pH 5.6 and 2 $^\circ\text{C}$. ^h Stereospecific assignments for Ni(II) UMC are as for *R. vernicifera* stellacyanin and M121Q azurin, which are consistent with the observed T_1 values of protons in Ni(II) UMC and metal proton distances in the structure of *C. sativus* stellacyanin.⁹ ⁱ A tentative assignment unsupported by NOE data.

two His ligands are affected to a lesser extent by the alkaline transition in Ni(II) UMC (see Table 4).

Discussion

The UV/vis spectrum of Cu(II) UMC is dominated by an intense $\text{S}(\text{Cys}) \rightarrow \text{Cu}(\text{II})$ LMCT band at 606 nm with a second weaker LMCT transition (also involving the Cys ligand) at 463 nm (see Figure S1). The low intensity of the 463 nm band, along with the axial EPR spectrum for the protein (see Figure S1), results in UMC being classified as having a classic type 1 copper site.³⁰ In most other stellacyanins, the LMCT band at ~450 nm is more intense and, along with their rhombic EPR spectra (see Figure S1), indicates the presence of perturbed type 1 copper centers.³⁰ The UV/vis spectrum of Ni(II) UMC is homologous to those of other Ni(II) cupredoxins (see Table 1), and the main $\text{S}(\text{Cys}) \rightarrow \text{Ni}(\text{II})$ LMCT band is found at 408 nm. A comparison of the data in Table 1 demonstrates that the spectrum of Ni(II) UMC resembles more closely those of Ni(II) *R. vernicifera* stellacyanin³⁸ and Met121Gln azurin,⁴⁰ which both possess axial Gln ligands (all of the other cupredoxins listed in Table 1 have an axial Met ligand). This is consistent with the active-site environment of UMC being very similar to those of other cupredoxins with an axial Gln ligand. There does not appear to be any discernible distinction between the UV/vis spectrum of Ni(II) UMC and the spectra of other Ni(II) stellacyanins along the lines of the differences seen for the Cu(II) proteins.

The assigned ^1H NMR spectra of Cu(II) and Ni(II) UMC provide detailed information about the coordination environment of the active site and the interaction of the paramagnetic metal ions with the ligands. Most of the isotropically shifted reso-

nances observed in the spectrum of Cu(II) UMC arise from the two His ligands, which is also true for the other proteins listed in Table 2. The positions of these resonances are remarkably similar in all three proteins, indicating that the spin density distribution onto these two ligands is homologous. This is also the case if cupredoxins, which possess an axial Met ligand, are included in this comparison.^{33,36,42–44} The backbone amide of the residue adjacent to the N-terminal His ligand (Asp45 in UMC²³) hydrogen bonds to the thiolate sulfur of the coordinated Cys in all known cupredoxin structures, resulting in the relatively large Fermi-contact shift of its C^αH proton resonance. The fact that this residue is an Asp in UMC, as compared to the Asn usually found in this position, has little effect on the interaction with the Cys ligand as the shift of peak g is similar to that observed in other cupredoxins including rusticyanin which has a Ser residue in this position.^{18,27,33,36,42–44} The C^αH proton of Cys85 (peak i) possesses negative spin density, and its resonance exhibits a very similar δ_{obs} value as compared to that seen in other cupredoxins.^{33,36,42–44} Although the significant δ_{obs} values of the two C^αH protons in the spectrum of Cu(II) UMC indicate considerable spin density on the Cys ligand, the δ_{Fc} values of these protons are not a good gauge of the strength of the Cu–S(Cys) bond in cupredoxins.⁴⁴ The shifts of the C^βH protons of Cys85 would provide more information about the spin density on this ligand in Cu(II) UMC, but these signals are too broad to be directly observed [attempts at 500 MHz to observe these resonances in Cu(II) UMC using indirect methods were unsuccessful]. The Cys C^βH protons are found at 450 and 375 ppm in the NMR spectrum of *C. sativus* stellacyanin.³³

The paramagnetic ¹H NMR spectrum of Cu(II) UMC does not contain any shifted resonances from the axial ligand. This is also the case in the spectrum of *C. sativus* stellacyanin where no resonances from the axial Gln ligand experience sizable Fermi-contact shifts.³³ This is consistent with the axial Gln ligand not contributing to the singly occupied molecular orbital (SOMO) in which the unpaired electron is located in *C. sativus* stellacyanin,³⁰ which must also be the case in UMC. Thus, the presence of a classic type 1 site in UMC (see Figure S1) does not alter this feature of the electronic structure as compared to other stellacyanins which have perturbed type 1 sites.^{15,18,28–31}

The ¹H NMR spectrum of Ni(II) UMC demonstrates that, as well as having two His ligands and a coordinated Cys, the active site of this protein is completed by an axial Gln ligand. The observation of the resonance from one of the N^ε2H protons of Gln95 (peak m) indicates that this residue coordinates to Ni(II) in a monodentate fashion via the side-chain carbonyl oxygen. Coordination through this atom results in the N^ε22H proton being only 3.13 Å from the metal and a distance of 4.52 Å between the N^ε21H proton and the metal [distances are taken from the crystal structure of *C. sativus* Cu(II) stellacyanin⁹ with protons added using Insight II]. If the Gln coordinated to the metal via its amide nitrogen, then this atom would have to be deprotonated. The remaining N^ε2H proton would be located very close to the metal and would have dramatically different relaxation properties than those observed for peak m. Thus, we assign resonance m as arising from the Gln95 N^ε21H proton. This is consistent with interproton distances in the structure of *C. sativus* stellacyanin and the NOE intensities that we observe (the Gln N^ε21H proton is 2.37 and 2.81 Å from the Gln C^γH protons, whereas the N^ε22H proton is 3.56 and 3.78 Å away⁹). This

conclusion is also supported by the observation that the N^ε21H proton of the axial Gln ligand points toward the indole ring of Trp13 in the *C. sativus* stellacyanin structure⁹ (this Trp is conserved in all known phytyocyanin sequences including that of UMC²³), explaining why this proton exchanges slowly with the bulk solvent (peak m is observed even at pH 10.7 and elevated temperature). The N^ε22H proton is close to the paramagnetic metal ion, and its resonance is consequently broadened beyond detection in the spectrum of Ni(II) UMC. The N^ε21H proton resonance of the axial Gln ligand is not observed in the NMR spectrum of Co(II) *R. vernicifera* stellacyanin²⁰ and has only been tentatively assigned in the spectrum of the Ni(II) protein.³⁴ The coordination mode of the axial Gln ligand determined herein for Ni(II) UMC is consistent with the electron paramagnetic resonance (EPR) parameters of the Cu(II) protein, which when put into a modified Vännegård–Peisach–Blumberg plot indicate coordination by an axial oxygen ligand.⁴⁵

The interpretation of the δ_{obs} values of the isotropically shifted resonances in the paramagnetic NMR spectrum of a Ni(II) cupredoxin is less straightforward than for the copper protein due to the greater magnetic anisotropy and thus more significant δ_{pc} contributions [see footnote b of Table 2]. To calculate the δ_{pc} contributions to the isotropic shifts requires that the orientation and components of the magnetic susceptibility (χ) tensor be known. These can only be determined if there is detailed three-dimensional structural information for the protein, which is presently not the case for UMC. In the case of Ni(II) azurin, the orientation and components of the χ -tensor have been determined and the δ_{pc} values are relatively small (the largest value being 17.0 ppm for one of the His ligand C^ε1H protons).⁴⁶ The orientation of the χ -tensor generates negative δ_{pc} contributions to the shifts of protons orientated toward the axial positions in Ni(II) azurin.⁴⁶ The temperature dependence of the δ_{obs} values for the protons listed in Table 2 (vide supra) indicates that the δ_{pc} contributions are not so significant for most signals in the NMR spectrum of Ni(II) UMC. Therefore, the δ_{obs} values are mainly dominated by the δ_{Fc} contributions and thus provide detailed information about metal–ligand interactions. Of particular interest is a comparison of the δ_{obs} values of Ni(II) UMC to those of other Ni(II) cupredoxins with an axial Gln ligand (see Table 4).^{34,40}

The shifts of the C^γ1H proton of the axial Gln ligand indicate appreciable spin density on this ligand in the Ni(II) proteins (the C^γH protons are four bonds away from the paramagnetic metal ion). This is contrary to the situation in the Cu(II) proteins where shifted resonances from the axial Gln are not observed outside of the diamagnetic envelope. Thus, in Ni(II) UMC, an orbital (presumably the d_{z²} orbital) possessing an unpaired electron is oriented toward the axial Gln ligand. The enhanced shift of the C^γ1H proton in Ni(II) UMC as compared to that in Ni(II) *R. vernicifera* stellacyanin could be indicative of increased spin density on the axial ligand, a slightly altered conformation of the Gln ligand, a modified orientation of the χ -tensor, or a combination of all of these factors. The negative shifts of the Gln C^γ2H proton in all of the proteins listed in Table 4 indicate that its δ_{Fc} value is considerably smaller than that for the C^γ1H

(45) Diederix, R. E. M.; Canters, G. W.; Dennison, C. *Biochemistry* **2000**, *39*, 9551–9560.

(46) Donaire, A.; Salgado, J.; Moratal, J. M. *Biochemistry* **1998**, *37*, 8659–8673.

proton and thus δ_{obs} is dominated by a negative δ_{pc} contribution [in Ni(II) azurin, the $\text{C}^{\gamma 2}\text{H}$ proton of the axial Met ligand possesses a negligible δ_{Fc} value⁴⁶]. The conclusion from the data in Table 4 therefore is that the Ni(II)–O(Gln) interaction is very similar in all of the proteins included and particularly in UMC and *R. vernicifera* stellacyanin.

The δ_{Fc} contributions to the shifts of the signals from the Cys C^{β}H protons are dependent upon the spin density on the thiolate sulfur of the Cys and also the Ni(II)– S^{γ} – C^{β} – H^{β} dihedral angles. The average shift of the resonances for these protons ($\delta_{\beta,\text{av}}$) is less sensitive to orientation effects than the separation between these signals and is thus a more useful measure of the spin density on the Cys ligand.³² The $\delta_{\beta,\text{av}}$ values are 190, 187, and 208 ppm for Ni(II) UMC, Ni(II) *R. vernicifera* stellacyanin,³⁴ and Ni(II) Met121Gln azurin,⁴⁰ respectively. Thus, all three Ni(II) proteins possess comparable spin densities on their Cys ligands. These $\delta_{\beta,\text{av}}$ values are significantly less than those seen in Ni(II) cupredoxins which have a weak axial Met ligand [values range from 210 ppm for Ni(II) azurin⁴⁰ to 285 ppm for Ni(II) pseudoazurin³⁵]. Therefore, the increased interaction of the metal with the axial Gln ligand results in a decrease in the Ni(II)–S(Cys) bond strength. A similar conclusion has been made from studies on Cu(II) stellacyanins which have an approximately 0.1 Å longer Cu(II)–S(Cys) bond as compared to those of other cupredoxins.⁴⁷ Recently, this relationship between the strength of the axial interaction and the Cu(II)–S(Cys) bond length has been further demonstrated in studies on wild-type *C. sativus* stellacyanin and its Gln99Met and Gln99Leu variants.³¹

The spin densities on the two His ligands at the active sites of Ni(II) UMC and Ni(II) *R. vernicifera* stellacyanin are remarkably similar. However, there are some differences between the two proteins in the behavior of the resonances belonging to the exchangeable protons of the coordinated imidazoles, with the signals from both His ligands observed at pH 6.5 in the spectrum of Ni(II) UMC. In the case of Ni(II) *R. vernicifera* stellacyanin, the corresponding signals are only observed at much lower pH values (and low temperatures).³⁴ A similar difference in behavior for the $\text{N}^{\epsilon 2}\text{H}$ protons of the two His ligands has been found in the Cu(II) proteins.^{18,26} This, along with the slow exchange of the Gln95 $\text{N}^{\epsilon 21}\text{H}$ proton, points to the active site of UMC being more buried than that of *R. vernicifera* stellacyanin.

The close homology of the δ_{obs} values observed in the paramagnetic ^1H NMR spectra of Cu(II) and Ni(II) UMC and *R. vernicifera* stellacyanin (see Tables 2 and 4) is surprising considering that the proteins have quite distinct UV/vis and EPR spectra (see Figure S1). The presence of either a classic or a perturbed type 1 copper site in cupredoxins possessing an axial Met ligand has been associated with alterations in the Cu–S(Met) interaction (perturbed sites possessing a stronger interaction).^{29,30} In the case of the Ni(II) stellacyanins, the axial Ni(II)–O(Gln) interaction is similar. In the native Cu(II) proteins, including *C. sativus* stellacyanin which is known to possess a Cu(II)–O(Gln) bond length of 2.21 Å,⁹ shifted resonances from the axial ligand are not observed. It seems likely that the

Cu(II)–O(Gln) bond length in Cu(II) UMC is similar to that in *C. sativus* stellacyanin and thus the active-site alterations which give rise to either classic or perturbed type 1 sites in stellacyanins are small and do not have a significant influence on their paramagnetic NMR spectra. Theoretical studies on models of type 1 copper sites have indicated that the energies of classic and perturbed centers are very similar. Thus, small differences in the protein fold of a particular cupredoxin may result in stabilization of either one of these active-site structures.^{48,49}

The reduction potential of UMC is 290 mV,²⁶ which falls within the normal range of values observed for cupredoxins. The stellacyanin from *R. vernicifera* has a much lower reduction potential of 185 mV,¹⁸ which has been attributed to the presence of a hard axial oxygen ligand.¹⁹ Given the similarity of the active-site structures of UMC and *R. vernicifera* stellacyanin, the axial ligand cannot be solely responsible for the low reduction potential in the latter. The studies described herein indicate decreased solvent accessibility of the active site of UMC as compared to *R. vernicifera* stellacyanin, which may contribute to its higher reduction potential. However, *C. sativus* stellacyanin appears to have a more exposed active site than UMC; yet it possesses a similar reduction potential (260 mV¹⁷). The factors controlling the reduction potentials of redox metalloproteins are complex, and recent theoretical studies have shown that the orientation of the protein permanent dipoles around the active site is a key factor.⁵⁰ A definitive answer on this subject must await more detailed structural information for UMC.

The alkaline transition results in a change in color of both Ni(II) and Cu(II) UMC. The ca. 10 nm shift in the LMCT bands observed upon raising the pH of Ni(II) UMC to 10.6 is significantly smaller than the 20 nm shift in the LMCT bands in the Cu(II) protein [in Cu(II) UMC, the S(Cys) → Cu(II) LMCT bands at 606 and 455 nm at neutral pH shift to 584 and 439 nm, respectively, at pH 11].²⁶ An even smaller influence of increasing pH on the UV/vis spectrum is seen for Co(II) *R. vernicifera* stellacyanin³² [we observe a larger effect on the UV/vis spectrum of Co(II) UMC, but this is also smaller than the changes seen in the Cu(II) protein – data not shown]. Therefore, the alkaline transition seems to have a more limited effect on metal-substituted UMCs as compared to the Cu(II) protein, but has a more significant influence on the metal center of UMC than that of *R. vernicifera* stellacyanin.

The effect of increasing pH on the δ_{obs} values of protons in Ni(II) UMC (see Table 4) provides detailed information about the influence of the alkaline transition on the active-site structure of this protein. The decrease in the $\delta_{\beta,\text{av}}$ value from 196 ppm at pH 8.0 to 170 ppm at pH 10.7 highlights a significant decrease in the Ni(II)–S(Cys) bond strength as a result of the alkaline transition. The diminished separation between the Cys85 C^{β}H proton resonances indicates that there is also a change in the conformation of this residue, affecting the H^{β} – C^{β} – S^{γ} –Ni(II) dihedral angles, at alkaline pH. The Ni(II)–O(Gln) interaction is also diminished as a consequence of the alkaline transition, but the observation of the Gln95 $\text{N}^{\epsilon 21}\text{H}$ proton resonance at

(47) DeBeer, S.; Randall, D. W.; Nersissian, A. M.; Valentine, J. S.; Hedman, B.; Hodgson, K. O.; Solomon, E. I. *J. Phys. Chem. B* **2000**, *104*, 10814–10819.

(48) Pierloot, K.; De Kerpel, J. O. A.; Ryde, U.; Olsson, M. H. M.; Roos, B. O. *J. Am. Chem. Soc.* **1998**, *120*, 13156–13166.

(49) De Kerpel, J. O. A.; Pierloot, K.; Ryde, U.; Roos, B. O. *J. Phys. Chem. B* **1998**, *102*, 4638–4647.

(50) Olsson, M. H. M.; Hong, G.; Warshal, A. J. *Am. Chem. Soc.* **2003**, *125*, 5025–5039.

pH 10.7 highlights that the coordination mode of the axial ligand is not altered at high pH. Electron nuclear double resonance studies previously suggested that the alkaline form of *R. vernicifera* stellacyanin involves coordination of the Gln ligand via its deprotonated side-chain amide nitrogen atom.⁵¹ Our data demonstrate that this is not the case in UMC, which is consistent with the results of a range of other investigations.^{45,52,53} The resonances from the two His ligands are also slightly shifted at high pH, and thus the alkaline transition affects all of the M(II)–ligand interactions at the active site of UMC. A similar conclusion has been made on the basis of paramagnetic NMR studies on the Cu(II) protein.²⁶ Paramagnetic NMR investigations on the influence of the alkaline transition in Co(II) *R. vernicifera* stellacyanin indicate a similar, but more limited, effect on the active-site structure.³² In conclusion, the active-site structural change which occurs as a consequence of the alkaline transition involves all of the coordinating residues in UMC. The main influence is on the axial ligand and the coordinating Cys with the strength of the bond to the latter decreasing considerably along with a change in the orientation of this ligand. These observations are consistent with the significant influence that the alkaline transition has on the S(Cys) → M(II) LMCT transitions in the UV/vis spectra of the proteins.^{18,26} The alkaline transition seems to have a greater effect on the active-site structure of UMC than in the case of *R. vernicifera* stellacyanin.

(51) Thomann, H.; Bernado, M.; Baldwin, M. J.; Lowery, M. D.; Solomon, E. *J. Am. Chem. Soc.* **1991**, *113*, 5911–5913.

(52) Romero, A.; Hoitink, C. W. G.; Nar, H.; Huber, R.; Messerschmidt, A.; Canters, G. W. *J. Mol. Biol.* **1993**, *229*, 1007–1021.

(53) Nersissian, A. M.; Nalbandyan, R. M. *Biochim. Biophys. Acta* **1988**, *957*, 446–453.

Conclusions

In this study, we have determined the active-site structure of UMC, the stellacyanin from horseradish roots. We have assigned the directly observed resonances in the paramagnetic ¹H NMR spectra of the native Cu(II) protein and also its Ni(II) derivative. Resonances from the axial Gln ligand are not shifted outside of the diamagnetic region in the Cu(II) protein but can be observed and assigned in Ni(II) UMC. These spectra demonstrate that UMC possesses the typical His₂Cys equatorial ligands with the axial Gln95 coordinating in a monodentate fashion via its side-chain amide oxygen atom. We assume that the axial ligand coordinates in a similar fashion in the Cu(II) protein.

The cupric site of UMC possesses a classic type 1 site, whereas almost all other stellacyanins have perturbed type 1 copper centers. The paramagnetic NMR studies described herein demonstrate that the active-site architectures of UMC and other stellacyanins are almost identical. Thus, subtle structural modifications must be responsible for the altered type 1 spectroscopic features seen in these proteins. The alkaline transition, which is observed in phytocyanins, affects all of the ligating residues but does not involve a change in coordination mode of the axial Gln ligand.

Acknowledgment. We thank BBSRC (grant no. 13/B16498) for funding and EPSRC for grants to purchase the NMR spectrometers.

Supporting Information Available: Experimental spectra (PDF). This material is available free of charge via the Internet at <http://pubs.acs.org>.

JA0375378